SUBDUCTION ZONE

Geochemical evidence for mélange melting in global arcs

Sune G. Nielsen[1,2]* and Horst R. Marschall[2,3]

In subduction zones, sediments and hydrothermally altered oceanic crust, which together form part of the subducting slab, contribute to the chemical composition of lavas erupted at the surface to form volcanic arcs. Transport of this material from the slab to the overlying mantle wedge is thought to involve discreet melts and fluids that are released from various portions of the slab. We use a meta-analysis of geochemical data from eight globally representative arcs to show that melts and fluids from individual slab components cannot be responsible for the formation of arc lavas. Instead, the data are compatible with models that first invoke physical mixing of slab components and the mantle wedge, widely referred to as high-pressure mélange, before arc magmas are generated.

INTRODUCTION

The physical processes that control mass transfer between subducted slab and the mantle wedge in subduction zones are critical for our understanding of volcanic arc formation and their associated earthquake and eruption hazards. In addition, these processes control the long-term transfer of water, carbon dioxide, and other volatiles from Earth's surface to the deep mantle, which has important implications for plate tectonics (*1*), long-term global climate (*2*), and the evolution of Earth's heat budget (*3*). However, the transport mechanisms of slab material to the mantle wedge remain a topic of significant debate (*4*–*8*), which renders our understanding of, for example, global volatile cycling highly uncertain. This is a problem, because interpretations of geochemical and geophysical data on subduction zones that are based on false geodynamic models must lead to erroneous conclusions and to fundamentally misguided constructs about how the crust is processed and recycled in modern plate tectonics. Subduction zones are the primary location where the crust interacts with the mantle, and all models on long-term crustal and mantle evolution, as well as short-term recycling and redistribution of volatiles, hinge on the accuracy of the used geodynamic model for these active plate margins.

Direct geophysical observations of sub-arc processes, however, presently lack the resolution to obtain fine-scale information about the material transfer processes at the slab-mantle interface. Therefore, the chemical and isotopic compositions of arc lavas offer the best opportunity to obtain information about this critical region of subduction zones. One of the most ubiquitous characteristics of arc lavas is the fractionation of several trace element ratios, such as Sr/Nd, Ba/Th, U/Nb, and Ce/Pb, compared with the ranges observed in all the slab components and the mantle wedge (*9*–*11*). These ratios are all essentially unperturbed by normal melting processes at mid-ocean ridges (*12*), and hence, any model of material transport from the slab to the mantle must also account for the generation of these trace element signatures.

Experimental work published over the past decade has shown that a combination of partial melting of subducted sediments and metamorphic dehydration of altered oceanic crust (AOC) has the ability to generate the required trace element fractionations (*8*, *13*, *14*). In particular, the stability of accessory minerals that sequester high concentrations of rare earth elements (REEs) during sediment melting can control the trace element ratios of the partial sediment melts (*8*, *14*, *15*). As a result, most studies of subduction zone processes infer that this metasomatized mantle model (Fig. 1A) is the primary vector for explaining material transfer between the slab and the mantle [for example, Ryan and Chauvel (*16*) and Schmidt and Poli (*17*)]. In detail, these models of slab-mantle interaction may also include fluid flux from dehydrating serpentinite in the lithospheric mantle of the subducting plate that either directly metasomatizes the mantle wedge or causes melting of sediments and/or AOC as the fluid ascends through the slab (*18*, *19*). However, a common trait that all of these models have in common is that the characteristic trace element fractionation of arc lavas is produced in the slab before mixing with the mantle wedge takes place.

Many field outcrops of exposed subducted oceanic material comprise rocks generally referred to as mélange. High-pressure mélanges consist of blocks of metaigneous, metasedimentary, and ultramafic materials embedded in newly formed hybrid rock types (chlorite-rich mélange matrix) that form as a product of high-strain mixing at the slab-mantle boundary during subduction (*5*). This mélange matrix has mechanical, thermodynamic, and geochemical properties that are entirely different compared with its contributing components: sediments, AOC, and mantle (*20*). Although mélanges often contain fragments of their precursor materials in field outcrops, the dominating mélange matrix is a separate lithology with distinct mineralogical, trace element, and isotopic characteristics (*5*). Mélange melting experiments have produced melts with a range in composition from basaltic to dacitic (and alkaline compositions) in equilibrium, with restitic mineral assemblages dominated by pyroxenes and, depending on pressure-temperature, olivine, garnet, spinel, amphibole, and/or phlogopite (*6*, *7*, *21*). Melting experiments on natural mélange rocks have also demonstrated that accessory minerals remain in the residue of mélange melts to temperatures up to 1150°C, and that they control trace element fractionations similar to those observed in sediment melting experiments (*21*). These particular experiments generated alkaline melt compositions from melting of one type of natural mélange rock, which represents only a subset of magmas observed in subduction zones. However, they demonstrate that mélange melting causes trace element fractionation, even at relatively high temperatures. This renders models involving mélange material produced at the top of the slab (Fig. 1B) equally compatible with the observed trace element signatures in arc lavas.

Physically, the two end-member models of slab material transport are very different (Fig. 1) and have very different consequences for the thermal structure and distribution of volcanoes in subduction zones

[1]NIRVANA Laboratories, Woods Hole Oceanographic Institution, Woods Hole, MA 02543, USA. [2]Department of Geology and Geophysics, Woods Hole Oceanographic Institution, Woods Hole, MA 02543, USA. [3]Institut für Geowissenschaften, Goethe Universität Frankfurt, Altenhöferalle 1, 60438 Frankfurt am Main, Germany.
*Corresponding author. Email: snielsen@whoi.edu

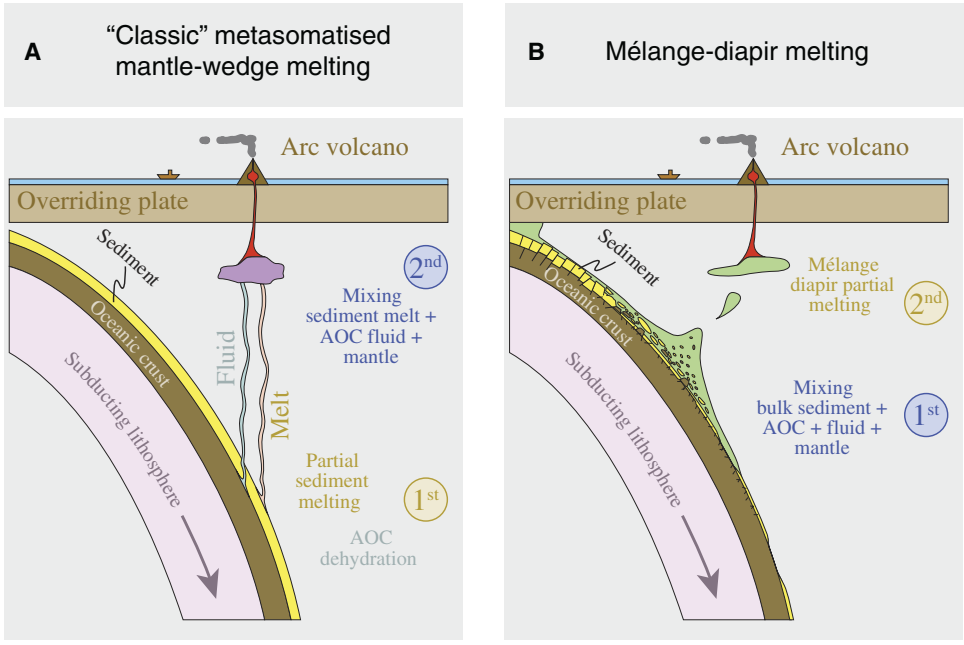

Fig. 1. Illustration of the two different end-member models of slab material transport in subduction zones. (**A**) In the conventional model, sediment melts and fluids from AOC, which both display fractionated trace element signatures, are sourced directly beneath the arc volcano, where they percolate rapidly to the region of melting. Here, they mix with ambient mantle melts to form arc magmas. (**B**) In the mélange model, sediments, AOC, and hydrated mantle physically mix to form hybrid mélange rocks. The mélange subsequently rises as diapirs into the mantle wedge and melts to form arc magmas with fractionated trace element signatures. The critical difference between the two models is that mixing and trace element fractionation for the two models occur in reverse order of each other, which will generate different isotopic mixing relationships. Illustration not to scale.

as well as chemical budgets of crustal cycling into the deep Earth. However, the chemical compositions of arc lavas predicted from both models will equally display fractionated trace element ratios, and both types of models also predict arc magmas that contain small amounts of subducted sediment and/or AOC components that can be detected using, for example, radiogenic isotope ratios, such as $^{87}Sr/^{86}Sr$ and $^{143}Nd/^{144}Nd$. The primary difference between the two end-member models of slab-to-mantle wedge material transport lies in the sequence of events that lead to the combination of the various components to form arc magmas. In the classic metasomatized mantle model with sediment melting and AOC and/or serpentinite dehydration, trace element fractionation occurs within the slab followed by mixing of these mobile components with the mantle wedge (Fig. 1A). In contrast, mélange models invoke physical mixing of the different bulk slab components first, followed by melting and dehydration processes that cause trace element fractionation (Fig. 1B). Hence, the succession of the two main events—mixing and melting—is exactly reversed in the mélange models compared to the classic metasomatized mantle melting models.

RESULTS

Discrimination of mélange melting and metasomatized mantle models

A very effective means of discriminating the two models is by using plots of $^{87}Sr/^{86}Sr$ versus $^{143}Nd/^{144}Nd$, because the elemental Nd/Sr ratios of bulk sediment and AOC are very different to those of sediment melts and AOC-derived fluids (*13*, *14*, *22*). In particular, both sediment melts and AOC fluids display much higher Sr/Nd than do their respective bulk counterparts. Therefore, mixing curves between the mantle and these components in Sr/Nd isotope space have very different curvature, which enables discrimination between arc magma sources that are dominated by the addition of melts and fluids from the slab and those dominated by mixing of bulk sediment (and bulk AOC) with the mantle. Figure 2 shows literature data from three different island arcs plotted in this type of isotope-isotope mixing diagram, where we explore the effects of sediment addition in arc lavas. Three different mixing lines (in black), which represent addition of bulk sediment and two different degrees of sediment melting, are plotted. In each case, the sediment compositions represent systematic studies of the average sediment subducting underneath each respective arc (see the Supplementary Materials). For all three arcs, as well as the Aleutians (*22*), Ryukyu, Scotia, Kurile, and Sunda arcs (fig. S1), lavas closely follow the mixing lines predicted by bulk sediment mixing. Essentially, none of the data are compatible with the sediment melt mixing lines.

DISCUSSION

An alternative interpretation of the Sr-Nd isotope plots would be if fluids that were released from the slab plotted at or very close to the mantle wedge composition, which requires that the oceanic crust had the same Sr-Nd isotope compositions as the mantle wedge (*22*). Because of the potentially small contrast in Nd/Sr between AOC fluids and sediment melts (*13*, *14*), the curvature of the mixing lines between these two components might resemble that of mixing between bulk sediments and the mantle wedge. The fluids could also originate from dehydrated serpentinite deeper in the subducted slab, in which case they would reequilibrate with AOC or induce sediment melting before entering the mantle wedge (*18*) and thus largely obtain the same Sr and Nd concentrations and isotope compositions as AOC fluids and sediment melts. Overall, the scenario of fluids with Sr and Nd isotope

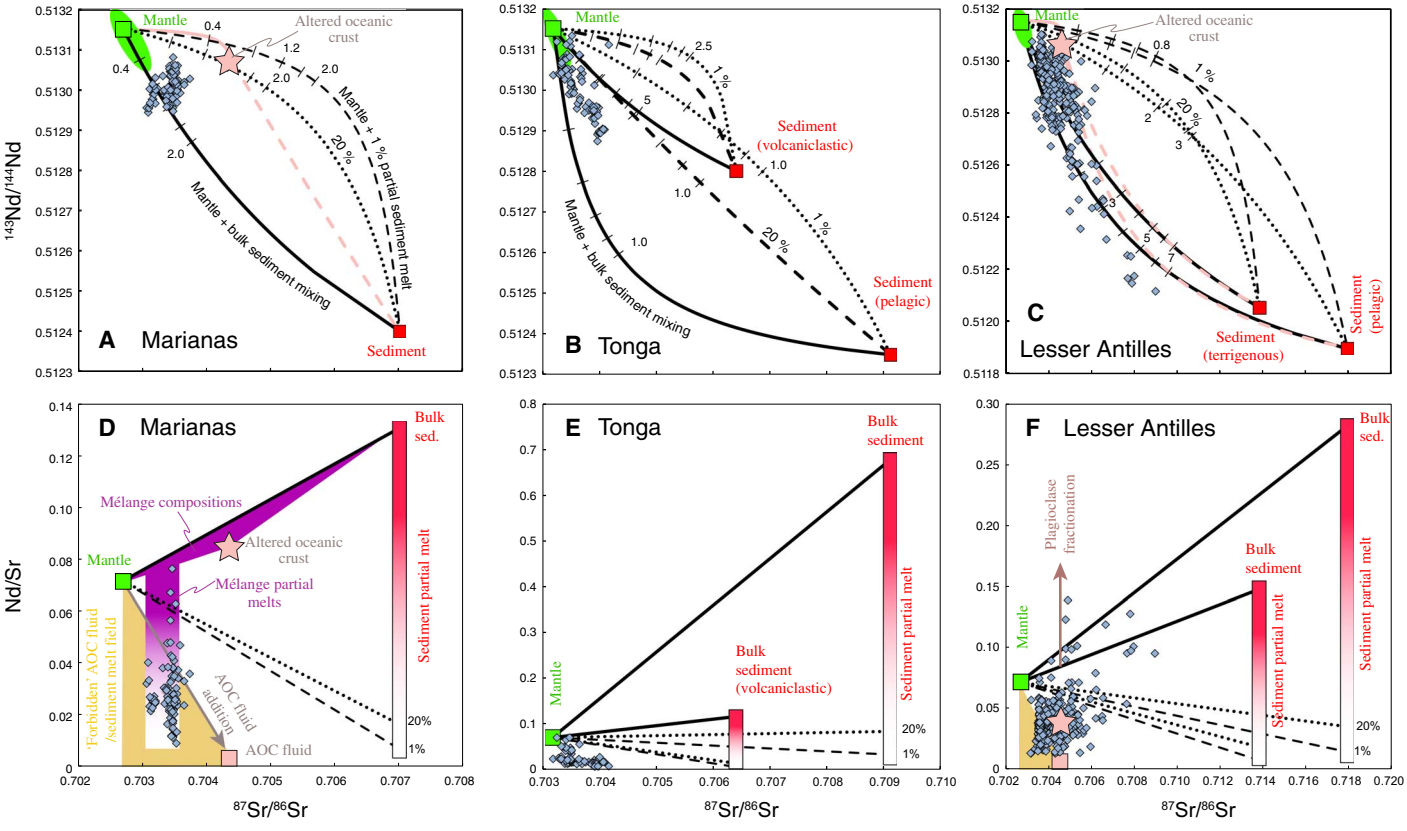

Fig. 2. Mixing diagrams between sediments and mantle for Tonga, Marianas, and Lesser Antilles arcs. Plots of Sr isotopes against Nd isotopes (**A** to **C**) and Nd/Sr ratio (**D** to **F**) for lavas from the Mariana (A and D), Tonga (B and E), and Lesser Antilles (C and F) arcs. Literature data from the GEOROC database (http://georoc.mpch-mainz.gwdg.de/georoc/) and only recent subaerial extrusive lavas with <62% SiO_2 have been included to avoid effects from fractional crystallization and assimilation (see the Supplementary Materials for details). Details of the mantle, sediment, and AOC end-member compositions can also be found in the Supplementary Materials. Mixing lines between the mantle and bulk sediment (black bold lines), 1% partial sediment melts (black dashed lines), and 20% partial sediment melts (black dotted lines) show different curvature, because Nd/Sr ratios fractionate strongly during sediment partial melting (*8*, *14*). Additional mixing lines between the mantle and AOC fluids (pink bold lines) and 1% partial sediment melts and 1% by weight AOC fluids (pink dashed lines) are also shown for arcs, where the AOC component is constrained (no AOC data exist for the Tonga arc). Tick marks on individual mixing curves indicate the amount of bulk sediment or sediment melt that is added to the mantle in weight percent. The partition coefficients for Sr and Nd during sediment melting were set to D_{Sr} = 7.3 and D_{Nd} = 0.35, respectively, which represent the average values recorded in sediment melting experiments by Hermann and Rubatto (*14*) over the temperature range of 750° to 900°C. Partition coefficients for AOC fluids were set to D_{Sr} = 2 and D_{Nd} = 0.15, which represent the values found for 800°C and 4 GPa (*13*). Arrows depict the effect on Nd/Sr and/or Nd and Sr isotopes during mélange partial melting (purple graded field), AOC fluid addition (gray arrow), and plagioclase fractional crystallization (brown arrow). Last, we also show a yellow shaded area, which depicts arc lava compositions that cannot be explained via addition of AOC fluids and sediment melts to the mantle wedge. The Nd/Sr ratios of AOC fluids in (D) and (F) are not quantified but conservatively inferred close to 0 to explore the largest possible effect from AOC fluid addition (see text for details).

compositions effectively identical to the mantle wedge could only occur if ocean crust alteration was minimal, thus causing only a negligible disturbance of the original unaltered oceanic crust Sr isotope composition [Nd isotopes are largely unaffected by hydrothermal alteration (*23*)]. Minor volumes of oceanic crust do display almost unaltered Sr isotope compositions (*24*, *25*), but more extensive alteration is always found in the shallowest portions of AOC (*24*, *25*), where fluids would ultimately have to pass through to enter the mantle wedge. Selective sampling of the unaltered portions of AOC is also not possible given that the most altered portions of oceanic crust display the most radiogenic Sr isotope compositions and have the highest water contents (*24*). Therefore, the Sr isotope composition of fluids that interacted with AOC would likely inherit the most radiogenic Sr isotope compositions found in AOC rather than the average value.

Average AOC subducting underneath the Marianas, Lesser Antilles, and Sunda arcs exhibits distinctly higher $^{87}Sr/^{86}Sr$ than the local mantle wedge, which would produce fluids with $^{87}Sr/^{86}Sr$ significantly higher than the mantle wedge. Therefore, mixing lines between sediment and AOC fluids only overlap with a minor fraction of arc lavas (Fig. 2 and fig. S1). In addition, mixing between the mantle, sediment melt, and AOC fluids only encompasses a minor fraction of the arc lava data because their Nd/Sr ratios are too low and, therefore, plot within a "forbidden zone" (Fig. 2, D to F). These considerations eliminate fluids from the slab as the component responsible for generating the observed Sr-Nd isotope curvature in these arcs. Given that AOC sections as young as 6 million years display strongly elevated $^{87}Sr/^{86}Sr$ (*24*, *25*), we conclude that fluids released from subducting slabs will not have Sr isotope compositions similar to unaltered mid-ocean ridge basalt, and therefore, addition of fluids is unable to explain any of the Sr-Nd isotope trends observed in arc lavas (Fig. 2 and fig. S1).

With these constraints, it follows that the Sr-Nd isotope systematics of the lavas in every one of the global range of arcs evaluated here adhere to mixing of the mantle with bulk sediment rather than sediment melts. Small variations in Sr and Nd isotope ratios may still be caused by

addition of AOC-derived fluids or sediment-derived melts due to inefficient mixing of the mélange layer at the top of the slab, but these are not major contributors. In addition, it is very likely that fluids released from metamorphic breakdown of hydrous minerals in the mélange itself play a role in arc magma generation. However, these processes must primarily take place after physical mixing of the different slab components and formation of mélange rocks has largely been completed.

The presence of sediment melts and AOC fluids has also been inferred based on diagrams in which radiogenic isotope ratios are plotted against elemental ratios, with the radiogenic element in the denominator (Fig. 3) (*26*, *27*). In these plots, mixing follows straight lines, and therefore, it is possible to make predictions that allow discrimination between the two end-member models of slab-to-mantle material transport (Fig. 3, B and C). Here, we use the Hf/Nd ratio, because both elements show low mobility in hydrous fluids (*13*), and the ratio is not fractionated during mantle melting or during fractional crystallization at early stages of magma differentiation (*12*). Therefore, variation in Nd isotopes should primarily relate to mixing of the mantle with either sediment melts or bulk sediment, whereas Hf/Nd fractionation may occur during either sediment or mélange melting.

Schematically, it is expected that mixtures of discreet sediment melts with the mantle wedge should produce magmas that fall along subvertical mixing lines, with variation in Nd isotopes and limited covariations of Hf/Nd ratios (Fig. 3B). Conversely, melting of mélange would produce magmas that fall on the bulk sediment-mantle mixing line, with an Nd isotope ratio determined by the relative proportions of the two components that formed the mélange. Subsequent Hf/Nd fractionation caused by mélange melting is expected to result in horizontal arrays with little variation in $^{143}Nd/^{144}Nd$ but a range of Hf/Nd ratios (Fig. 3C). In arcs, such as Tonga (Fig. 3A), the Aleutians (*28*), and the Marianas (*10*), it is common that individual volcanic centers display very limited radiogenic isotopic variation, whereas trace element ratios are highly variable. These characteristic trends are difficult to account for with sediment melt addition to a mantle source (Fig. 3B), but are readily explained with melting of an isotopically homogeneous mélange source underneath each volcanic center that melts to varying degrees, thus generating trace element fractionation (Fig. 3C).

The crucial difference between the two models lies in the relative timing of mixing and melting that independently affect isotope and trace element ratios, respectively. Addition of slab-derived sediment melts to the mantle source of arc magmas entails melting and trace element fractionation before mixing. In contrast, mélange melting implies that the components are first mixed to form a new hybrid rock, whereby their radiogenic isotope composition is set, and melted in the second step, whereby the trace elements may be fractionated. The horizontal arrays observed in Fig. 3A strongly support the latter model.

On the basis of simple sediment-mantle mixing lines (Fig. 2, A to C, and fig. S2), most arc magmas are predicted to only contain up to a few weight percent of sediment. It is possible that these small amounts of sediment would not be sufficient to stabilize the accessory minerals rutile, zircon, apatite, and monazite that can produce the characteristic trace element fractionation observed in arc lavas (*8*, *14*). However, as observed in experiments with natural mélange (*21*, *29*), a significant oceanic crust component is sufficient to produce accessory minerals, such as rutile and zircon, and REE-bearing minerals of the perovskite supergroup that generate the required trace element fractionation. Addition of a substantial AOC component within mélange would not significantly perturb the Nd-Sr mixing relationships because of the similar Sr and Nd isotopic compositions of oceanic crust and mantle relative to sediments. Hence, the minor sediment component in many mélanges (*5*) that is also mirrored by the amounts of sediment in global arcs (Fig. 2 and fig. S1) does not preclude accessory phase

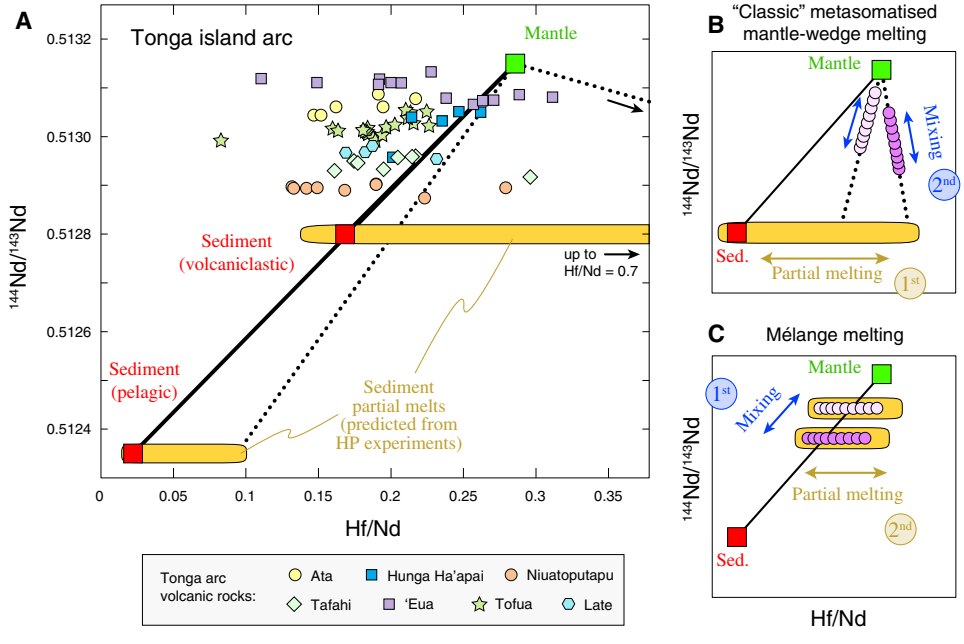

Fig. 3. Plot of Nd isotopes versus Hf/Nd ratios for lavas from the Tonga arc. (**A**) Literature data are from the GEOROC database (http://georoc.mpch-mainz.gwdg.de/georoc/). Mixing lines between the mantle and bulk sediment (bold lines) and between the mantle and sediment melts (dotted lines) are shown as examples. The yellow bar illustrates the range of sediment melts possible for sediment melting down to a degree of as little as 1%. Sediment melts were computed by using relative partition coefficients of Nd and Hf (D_{Nd}/D_{Hf} = 0.9 to 4.3) in accordance with the experimental range observed (*14*). Both Hf and Nd are immobile in AOC fluids (*13*), which render sediments the most likely source of variation in Hf/Nd. Therefore, no fluid component is plotted in the figure. Schematic illustrations of expected trends when (**B**) sediment melting is followed by mixing and (**C**) mélange formation is followed by melting are also shown.

formation and trace element fractionation, if the mélange also contains a substantial AOC component.

Mélange melting in different locations

Transfer of mélange material into the mantle wedge could occur via diapirs that rise buoyantly from the slab surface and partially melt in the hot corner of the mantle wedge (*5*, *7*). However, diapir formation in itself depends on the temperature, viscosity, and thickness of the buoyant layer (*4*), and it is likely that diapir formation may be inhibited in some arcs. In these cases, mélange material would likely be dragged down to greater depths, causing serpentine breakdown (*30*, *31*) and eventual melting of chlorite-rich schist at temperatures in excess of 800°C (*30*, *32*). The pressure conditions prevailing at the top of the slab are expected to stabilize garnet in the residue of these mélange melts (*6*, *7*, *32*). Hence, mélange melting at the top of the slab would potentially record residual garnet signatures, such as high Sr/Y and heavy REE depletions. Although not common, rocks with this type of chemical signature are found in many arcs (*33*). Classically, residual garnet signatures in arc lavas have been interpreted to reflect melting of the subducted basaltic crust at high pressure (*34*). However, this process is not expected for normal subduction processes and probably requires special circumstances or slab geometries (*35*). We speculate that mélange melting might be an alternative pathway to generate garnet signatures in subduction zone magmas. Conversely, the large dominance of arc rocks that lack any garnet signature requires that most mélange melting has to take place at pressures below approximately 2 GPa, where garnet is not part of the restitic mineral assemblage of mélange melting (*6*, *7*, *21*, *29*). This pressure equates to ≤60-km depth, and the slab surface is too cold at these shallow depths to cause any melting (*36*). Consequently, the mélange material can only melt if it is transported into hotter regions of the mantle wedge, and wedge diapirs are an appropriate mechanism to fulfill this task (*5*–*7*). Hence, REE signatures in arc magmas can be used to distinguish between melting of dragged-down mélange close to the slab-mantle interface and melting of mélange diapirs in the hot corner of the mantle wedge.

CONCLUSIONS AND OUTLOOK

It follows from the Nd-Sr isotope and Sr-Nd-Hf trace element ratios that bulk mixing of solid components along the slab-mantle interface—high-pressure mélange formation—is the main mechanism to determine the source composition of arc magmas. The significant difference in pressure expected for different mélange melting scenarios facilitates REE patterns and Sr/Y ratios as geochemical tools to distinguish melting near the slab surface from melting in mantle wedge diapirs. Generation of arc magmas by melting of mélange in diapirs or at the slab surface has consequences for the interpretation of geochemical data. Classical interpretations that draw conclusions from trace element signatures for apparent dehydration and melting processes in the slab and for its thermal structure are rendered invalid, if the magmas and their geochemical patterns are generated in mélange diapirs within the mantle wedge or mélange melting at the slab surface. Mélange rocks are rich in volatile elements; may act as a temporary storage of H_2O, CO_2, and sulfur near or at the slab surface; and control the volatile transport into the mantle wedge and into the deep mantle. The differences in the pathways and budgets of volatiles between the two contrasting models for the generation of arc magmas are drastic and call for a reevaluation of further published data sets and revision of concepts and conclusions on subduction zone processes.

MATERIALS AND METHODS

We used data for arc lavas compiled from the GEOROC database (http://georoc.mpch-mainz.gwdg.de/georoc/) for eight well-studied island arcs. Data were modeled using experimental element partitioning data for sediment melting and AOC fluid release (*13*, *14*).

SUPPLEMENTARY MATERIALS

Supplementary material for this article is available at http://advances.sciencemag.org/cgi/content/full/3/4/e1602402/DC1

Supplementary Text

fig. S1. Mixing diagrams between sediments and mantle for Kurile, Ryukyu, Scotia, Aleutian, and Sunda arcs.

fig. S2. Plots of SiO_2 against Sr isotopes for arc lavas from all eight arcs investigated in this study.

table S1. Compositions of endmember mixing components in Fig. 2 and fig. S1.

table S2. Strontium and neodymium isotope compositions for sediments and altered basalts in front of the Ryukyu arc.

References (*37*–*56*)

REFERENCES AND NOTES

1. C. O'neill, A. M. Jellinek, A. Lenardic, Conditions for the onset of plate tectonics on terrestrial planets and moons. *Earth Planet. Sci. Lett.* **261**, 20–32 (2007).
2. D. E. Canfield, The evolution of the Earth surface sulfur reservoir. *Am. J. Sci.* **304**, 839–861 (2004).
3. R. K. O'Nions, E. R. Oxburgh, Heat and helium in the Earth. *Nature* **306**, 429–431 (1983).
4. M. D. Behn, P. B. Kelemen, G. Hirth, B. R. Hacker, H.-J. Massonne, Diapirs as the source of the sediment signature in arc lavas. *Nat. Geosci.* **4**, 641–646 (2011).
5. H. R. Marschall, J. C. Schumacher, Arc magmas sourced from mélange diapirs in subduction zones. *Nat. Geosci.* **5**, 862–867 (2012).
6. A. Castro, T. Gerya, A. García-Casco, C. Fernández, J. Díaz-Alvarado, I. Moreno-Ventas, I. Löw, Melting relations of MORB–sediment mélanges in underplated mantle wedge plumes; implications for the origin of Cordilleran-type batholiths. *J. Petrol.* **51**, 1267–1295 (2010).
7. A. Castro, T. V. Gerya, Magmatic implications of mantle wedge plumes: Experimental study. *Lithos* **103**, 138–148 (2008).
8. S. Skora, J. Blundy, High-pressure hydrous phase relations of radiolarian clay and implications for the involvement of subducted sediment in arc magmatism. *J. Petrol.* **51**, 2211–2243 (2010).
9. J. A. Pearce, D. W. Peate, Tectonic implications of the composition of volcanic arc magmas. *Annu. Rev. Earth Planet. Sci.* **23**, 251–285 (1995).
10. T. Elliott, T. Plank, A. Zindler, W. White, B. Bourdon, Element transport from slab to volcanic front at the Mariana arc. *J. Geophys. Res. Solid Earth* **102**, 14991–15019 (1997).
11. M. T. McCulloch, J. A. Gamble, Geochemical and geodynamical constraints on subduction zone magmatism. *Earth Planet. Sci. Lett.* **102**, 358–374 (1991).
12. A. Gale, C. A. Dalton, C. H. Langmuir, Y. J. Su, J.-G. Schilling, The mean composition of ocean ridge basalts. *Geochem. Geophys. Geosyst.* **14**, 489–518 (2013).
13. R. Kessel, M. W. Schmidt, P. Ulmer, T. Pettke, Trace element signature of subduction-zone fluids, melts and supercritical liquids at 120–180 km depth. *Nature* **437**, 724–727 (2005).
14. J. Hermann, D. Rubatto, Accessory phase control on the trace element signature of sediment melts in subduction zones. *Chem. Geol.* **265**, 512–526 (2009).
15. K. Klimm, J. D. Blundy, T. H. Green, Trace element partitioning and accessory phase saturation during H_2O-saturated melting of basalt with implications for subduction zone chemical fluxes. *J. Petrol.* **49**, 523–553 (2008).
16. J. G. Ryan, C. Chauvel, in *Treatise on Geochemistry*, H. D. Holland, H. K. Turekian, Eds. (Elsevier, ed. 2, 2014), pp. 479–508.
17. M. W. Schmidt, S. Poli, in *Treatise on Geochemistry*, K. K. Turekian, Ed. (Elsevier, ed. 2, 2014), pp. 669–701.
18. L. H. Rupke, J. P. Morgan, M. Hort, J. A. D. Connolly, Serpentine and the subduction zone water cycle. *Earth Planet. Sci. Lett.* **223**, 17–34 (2004).
19. P. Ulmer, V. Trommsdorff, Serpentine stability to mantle depths and subduction-related magmatism. *Science* **268**, 858–861 (1995).
20. G. E. Bebout, Metamorphic chemical geodynamics of subduction zones. *Earth Planet. Sci. Lett.* **260**, 373–393 (2007).
21. A. M. Cruz-Uribe, H. Marschall, G. A. Gaetani, Arc magma genesis from melting of mélange diapirs, paper presented at the AGU Fall Meeting, San Francisco, CA, 17 December 2015.
22. S. G. Nielsen, G. Yogodzinski, J. Prytulak, T. Plank, S. M. Kay, R. W. Kay, J. Blusztajn, J. D. Owens, M. Auro, T. Kading, Tracking along-arc sediment inputs to the Aleutian arc using thallium isotopes. *Geochim. Cosmochim. Acta* **181**, 217–237 (2016).

23. M. T. Mcculloch, R. T. Gregory, G. J. Wasserburg, H. P. Taylor Jr., A neodymium, strontium, and oxygen isotopic study of the Cretaceous Samail Ophiolite and implications for the petrogenesis and seawater-hydrothermal alteration of oceanic-crust. *Earth Planet. Sci. Lett.* **46**, 201–211 (1980).
24. D. A. H. Teagle, J. C. Alt, W. Bach, A. N. Halliday, J. Erzinger, Alteration of upper ocean crust in a ridge-flank hydrothermal upflow zone: Mineral, chemical, and isotopic constraints from hole 896A. *Proc. Ocean Drill. Program Sci. Results* **148**, 119–150 (1996).
25. D. A. H. Teagle, J. C. Alt, A. N. Halliday, Tracing the chemical evolution of fluids during hydrothermal recharge: Constraints from anhydrite recovered in ODP Hole 504B. *Earth Planet. Sci. Lett.* **155**, 167–182 (1998).
26. C. Class, D. M. Miller, S. L. Goldstein, C. H. Langmuir, Distinguishing melt and fluid subduction components in Umnak Volcanics, Aleutian Arc. *Geochem. Geophys. Geosyst.* **1**, 1004 (2000).
27. D. M. Miller, S. L. Goldstein, C. H. Langmuir, Cerium/lead and lead isotope ratios in arc magmas and the enrichment of lead in the continents. *Nature* **368**, 514–520 (1994).
28. P. B. Kelemen, G. M. Yogodzinski, D. W. Scholl, Along-strike variation in lavas of the Aleutian Island Arc: Implications for the genesis of high Mg# Andesite and the continental crust, in *Inside the Subduction Factory: American Geophysical Union Monograph*, J. Eiler, Ed. (American Geophysical Union, 2003), vol. 138, pp. 223–311.
29. A. M. Cruz-Uribe, H. R. Marschall, G. A. Gaetani, N. G. Grozeva, Arc magma genesis from melting of mélange diapirs, paper presented at the Goldschmidt Conference, Prague, Czech Republic, 17 December 2015.
30. T. L. Grove, C. B. Till, E. Lev, N. Chatterjee, E. Médard, Kinematic variables and water transport control the formation and location of arc volcanoes. *Nature* **459**, 694–697 (2009).
31. M. W. Schmidt, S. Poli, Experimentally based water budgets for dehydrating slabs and consequences for arc magma generation. *Earth Planet. Sci. Lett.* **163**, 361–379 (1998).
32. T. L. Grove, N. Chatterjee, S. W. Parman, E. Médard, The influence of H_2O on mantle wedge melting. *Earth Planet. Sci. Lett.* **249**, 74–89 (2006).
33. H. Martin, Adakitic magmas: Modern analogues of Archaean granitoids. *Lithos* **46**, 411–429 (1999).
34. M. J. Defant, M. S. Drummond, Derivation of some modern arc magmas by melting of young subducted lithosphere. *Nature* **347**, 662–665 (1990).
35. G. M. Yogodzinski, J. M. Lees, T. G. Churikova, F. Dorendorf, G. Wöerner, O. N. Volynets, Geochemical evidence for the melting of subducting oceanic lithosphere at plate edges. *Nature* **409**, 500–504 (2001).
36. E. M. Syracuse, P. E. van Keken, G. A. Abers, The global range of subduction zone thermal models. *Phys. Earth Planet. In.* **183**, 73–90 (2010).
37. T. Plank, C. H. Langmuir, The chemical composition of subducting sediment and its consequences for the crust and mantle. *Chem. Geol.* **145**, 325–394 (1998).
38. J. D. Vervoort, T. Plank, J. Prytulak, The Hf–Nd isotopic composition of marine sediments. *Geochim. Cosmochim. Acta* **75**, 5903–5926 (2011).
39. A. Ewart, K. D. Collerson, M. Regelous, J. I. Wendt, Y. Niu, Geochemical evolution within the Tonga–Kermadec–Lau Arc–Back-arc systems: The role of varying mantle wedge composition in space and time. *J. Petrol.* **39**, 331–368 (1998).
40. V. J. M. Salters, A. Stracke, Composition of the depleted mantle. *Geochem. Geophys. Geosyst.* **5**, Q05B07 (2004).
41. F. E. Jenner, H. S. C. O'Neill, Analysis of 60 elements in 616 ocean floor basaltic glasses. *Geochem. Geophys. Geosyst.* **13**, Q02005 (2012).
42. C. M. Meyzen, J. Blichert-Toft, J. N. Ludden, E. Humler, C. Mével, F. Albarède, Isotopic portrayal of the Earth's upper mantle flow field. *Nature* **447**, 1069–1074 (2007).
43. G. M. Yogodzinski, S. T. Brown, P. B. Kelemen, J. D. Vervoort, M. Portnyagin, K. W. W. Sims, K. Hoernle, B. R. Jicha, R. Werner, The role of subducted basalt in the source of Island Arc Magmas: Evidence from Seafloor Lavas of the Western Aleutians. *J. Petrol.* **56**, 441–492 (2015).
44. E. Hegner, M. Tatsumoto, Pb, Sr, and Nd isotopes in basalts and sulfides from the Juan de Fuca Ridge. *J. Geophys. Res. Solid Earth Planets* **92**, 11380–11386 (1987).
45. D. Ben Othmann, W. M. White, J. Patchett, The geochemistry of marine sediments, island arc magma genesis, and crust-mantle recycling. *Earth Planet. Sci. Lett.* **94**, 1–21 (1989).
46. H. Staudigel, G. R. Davies, S. R. Hart, K. M. Marchant, B. M. Smith, Large scale isotopic Sr, Nd and O isotopic anatomy of altered oceanic crust: DSDP/ODP sites 417/418. *Earth Planet. Sci. Lett.* **130**, 169–185 (1995).
47. F. Hauff, K. Hoernle, A. Schmidt, Sr-Nd-Pb composition of Mesozoic Pacific oceanic crust (Site 1149 and 801, ODP Leg 185): Implications for alteration of ocean crust and the input into the Izu-Bonin-Mariana subduction system. *Geochem. Geophys. Geosyst.* **4**, 8913 (2003).
48. A. M. Volpe, J. D. Macdougall, G. W. Lugmair, J. W. Hawkins, P. Lonsdale, Fine-scale isotopic variation in Mariana Trough basalts: Evidence for heterogeneity and a recycled component in backarc basin mantle. *Earth Planet. Sci. Lett.* **100**, 251–264 (1990).
49. R. F. Gribble, R. J. Stern, S. H. Bloomer, D. Stüben, T. O'Hearn, S. Newman, MORB mantle and subduction components interact to generate basalts in the southern Mariana Trough back-arc basin. *Geochim. Cosmochim. Acta* **60**, 2153–2166 (1996).
50. R. Shinjo, J. D. Woodhead, J. M. Hergt, Geochemical variation within the northern Ryukyu Arc: Magma source compositions and geodynamic implications. *Contrib. Mineral. Petrol.* **140**, 263–282 (2000).
51. S. Fretzdorff, R. A. Livermore, C. W. Devey, P. T. Leat, P. Stoffers, Petrogenesis of the back-arc east Scotia Ridge, South Atlantic Ocean. *J. Petrol.* **43**, 1435–1467 (2002).
52. I. G. N. Silva, D. Weis, J. S. Scoates, J. Barling, The Ninetyeast Ridge and its relation to the Kerguelen, Amsterdam and St. Paul hotspots in the Indian Ocean. *J. Petrol.* **54**, 1177–1210 (2013).
53. D. Weis, F. A. Frey, A. Saunders, I. Gibson, Ninetyeast Ridge (Indian-Ocean): A 5000 km record of a Dupal mantle plume. *Geology* **19**, 99–102 (1991).
54. F. A. Frey, D. Weis, Temporal evolution of the Kerguelen plume: Geochemical evidence from 38 to 82 Ma lavas forming the Ninetyeast Ridge. *Contrib. Mineral. Petrol.* **121**, 12–28 (1995).
55. J. A. Pearce, P. D. Kempton, J. B. Gill, Hf–Nd evidence for the origin and distribution of mantle domains in the SW Pacific. *Earth Planet. Sci. Lett.* **260**, 98–114 (2007).
56. J. M. Hergt, J. D. Woodhead, A critical evaluation of recent models for Lau–Tonga arc-backarc basin magmatic evolution. *Chem. Geol.* **245**, 9–44 (2007).

Acknowledgments: We thank N. Shimizu, V. Le Roux, A. Cruz-Uribe, O. Jagoutz, J. Blusztajn, and G. Gaetani for discussions and B. Schoene and T. Sisson for constructive and insightful reviews. **Funding:** This work was supported by the NSF (EAR-1119373 to S.G.N., EAR-1427310 to S.G.N. and H.R.M., and EAR-1348063 to H.R.M. and G. Gaetani) and Woods Hole Oceanographic Institution–Ocean Exploration Institute (to H.R.M. and G. Gaetani). **Author contributions:** S.G.N. and H.R.M. conceived the project; S.G.N. performed all modeling and calculations; S.G.N. and H.R.M. wrote the manuscript. **Competing interests:** The authors declare that they have no competing interests. **Data and materials availability:** All data needed to evaluate the conclusions in the paper are present in the paper and/or the Supplementary Materials. Additional data related to this paper may be requested from the authors.

Submitted 29 September 2016
Accepted 16 February 2017
Published 7 April 2017
10.1126/sciadv.1602402

Citation: S. G. Nielsen, H. R. Marschall, Geochemical evidence for mélange melting in global arcs. *Sci. Adv.* **3**, e1602402 (2017).

Science Advances

Geochemical evidence for mélange melting in global arcs

Sune G. Nielsen and Horst R. Marschall

Sci Adv **3** (4), e1602402.
DOI: 10.1126/sciadv.1602402